



International Journal of Advanced Research in Electrical, Electronics and Instrumentation Engineering

(An ISO 3297: 2007 Certified Organization)

Website: www.ijareeie.com

Vol. 6, Issue 5, May 2017

A Three-Port DC–DC Converter for Stand-Alone Wind/Battery/PV Hybrid Systems to DC Loads

Daniyakula Veera Manikanta¹, K.Muni Pratap²

PG Student(PE), Dept. of EEE, AIMS college of Engineering, Andhra Pradesh, India¹

Associate Professor, Dept. of EEE, AIMS college of Engineering, Andhra Pradesh, India²

ABSTRACT: A three-port dc–dc convertor integration wind,pv and battery power for prime increase applications is planned during this paper. The topology includes 5 power switches, 2 coupled inductors, and 2 active-clamp circuits connected to wind-battery-PV hybrid system. The coupled inductors ar accustomed to attain high increase voltage gain and to scale back the voltage stress of input aspect switches. 2 sets of active-clamp circuits are accustomed recycle the energy holds on within the discharge inductors and to boost the system potency. The operation mode doesn't have to be compelled to be modified once a transition between charging and discharging happens. Moreover, trailing most electrical outlet of the windmill and PV power regulation the output voltage will be operated at the same time throughout charging/discharging transitions. As long because the wind speed and solar irradiation level isn't too low, the utmost power trailing (MPT) algorithmic rule are going to be disabled only if the battery charging voltage is just too high. Therefore, the control theme of the planned convertor provides most utilization of alternative energy most of the time. As a result, the planned convertor has deserves of high boosting level, reduced range of devices, and straightforward control strategy. The higher than explained system is going to be developed exploitation to Matlab/Simulink and therefore the results ar shown.

KEYWORDS: DCloads, energy storage, high step-up application, hybrid power system, wind source,pv three-port converter.

I.INTRODUCTION

INTEGRATED multiport converters for interfacing many power sources and storage devices area unitwideutilized in recent years. rather thanmistreatment individual power electronic converters for every of the energy sources, multiport converters have the benefitstogether with less elements, lower cost, a lot of compact size, and higher dynamic performance. In several cases, a minimum of one energy storage deviceought to be incorporated. as an example, within theelectrical vehicle application, the regenerative energy happensthroughout acceleration or start-up. Therefore, it'simportant for the port connected to the energy storage to permittwo-way power flow.

Various styles of topologies areplannedthanks tothe benefits of multiport converters. The mixturemethods for the multiport convertorembody sharing switches, capacitors, inductors, or magnetic cores [1]. One mightchoosea correct topology by considering several aspects likevalue, reliableness, and adaptabilitylooking on the applications. AN application ofhybrid energy offermistreatment renewable energy sources and storage devices is shown in Fig. 1. The dc microgrid enabled by the solid-state transformer (SST) within the Future Renewable electrical Energy Delivery and Management System (FREEDM System) integrates varied distributed renewable energy resources (DRERs) and distributed energy storage devices (DESDs) [2]. for example, if alternative energyiis chosenbecause the renewable energy supply and battery because thestorage device, the battery will either offer the load with the wind energy at constant time or store the surplus power from the aerogenerator for backup use. Therefore, the two-way power path should be provided for the battery port. The dc–dc converters interfacing the DRERs or DESDs area unit expected to own relative high voltage conversion ratios since the dc bus of the FREEDM system is 380 V. it's studied that for the Ac–dc and dc–dc converters connected to the wind generators and pv panels, voltage gain extension cells like coupled inductors, transformers, and switched capacitors artypicallyusedto realize high voltage conversion ratios [3]. By utilizing the voltage gain extension cells, the intense duty cycles that exist in typical boost converters will be avoided

International Journal of Advanced Research in Electrical, Electronics and Instrumentation Engineering

(An ISO 3297: 2007 Certified Organization)

Website: www.ijareeie.com

Vol. 6, Issue 5, May 2017

and also the voltage stress on switches will be reduced. Thus, power switches with lower voltage rating and lower input resistance will be chosen for the converters to scale back conductivity losses. A convertorexploitation coupled inductors is comparatively higher than isolation transformers since the coupled inductors have less complicated winding structure and lower conductivity loss [4]. However, the outflow inductors of the coupled inductors can consume important energy for an outsized winding quantitative relation. In such case, the voltage stress and also the loss of the switches can each be exaggerated. a liftdevice with coupled inductance and active-clamp circuit is planned in [4]. This boost device will yield a high change of magnitude voltage gain, scale back the voltage stress on switches, and recycle the energy within the outflow inductance.

Many multiport device topologies are given within the literature and might be roughly divided into 2 classes. One is no isolated sort [5]–[13]: the nonisolated converters are units sometimes derived from the standard buck, boost, or buck-boost topologies and are a lot of compact in size. the opposite is isolated sort [14]–[24]: the isolated converters mistreatment bridge topologies and multiwinding transformers to match wide input voltage ranges. In this paper, a high change of magnitude three-port dc-dc device for the hybrid wind/battery system is planned with the subsequent advantages: 1) high voltage conversion quantitative relation is achieved by mistreatment coupled inductors; 2) easy converter topology that has reduced range of the switches and associate circuits; 3) easy management strategy that doesn't have to be compelled to modification the operation mode when a charging/discharging transition happens unless the charging voltage is simply too high; and 4) output voltage is usually regulated at 380 V underneath all operation modes. it's noted that for the MPP-tracking converters, operational vary must be restricted to the voltage but the MPP voltage once the output voltage or current control is active [26]. This issue may be addressed by limiting the operative vary of the device within the voltages beyond MPP.

As shown in Fig. 1, examination to the standard multiconverter configuration with centralized control for the planned converter. Therefore, the system value and volume will be reduced. the most important contribution of this paper is to propose AN integrated three-port device as a non isolated various aside from typical isolated topologies for top change of magnitude three-port applications. The planned change strategy permits the device to be controlled by constant 2 duty cycles in several operation modes. The careful analysis is given within the following sections: The principle of operation is represented in Section II. The wind supply modelling, topological modes, and ZVS conditions are analysed in Section III. The modelling and control strategy is explained in Section IV. Finally, the simulation results are given in Section V

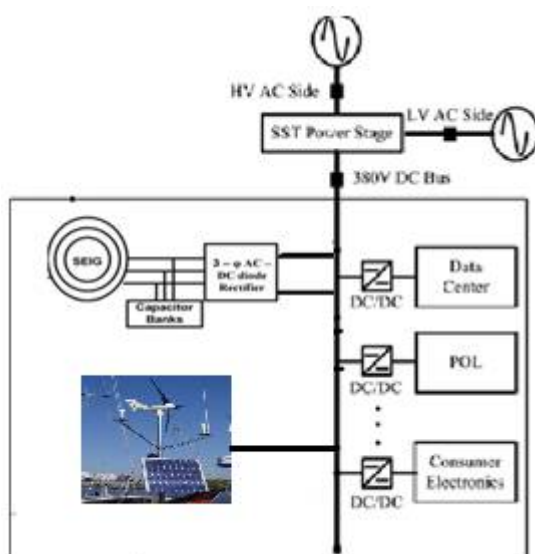


Figure:1 part of DC Micro grid

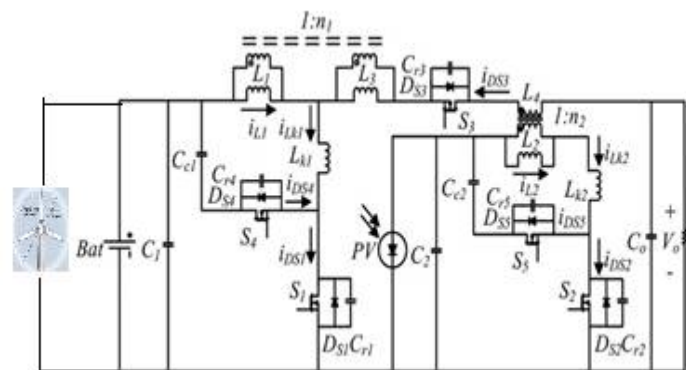


Figure 2: Topology of proposed converter



International Journal of Advanced Research in Electrical, Electronics and Instrumentation Engineering

(An ISO 3297: 2007 Certified Organization)

Website: www.ijareeie.com

Vol. 6, Issue 5, May 2017

II. PRINCIPLE OF OPERATION

This section introduces the topology of planned nonisolated three-port dc–dc convertor, as illustrated in Fig. 2. The convertor consists of 2 main switches S1 and S2 for the wind/battery and PV port. Synchronous switch S3 is driven complementarily to S1 specified bidirectional power flow for the battery port may be achieved. 2 coupled inductors with winding ratios n1 and n2 ar used as voltage gain extension cells. 2 sets of activeclampcircuitsformedbyS4,Lk1, Cc1 andS5, Lk2, Cc2 areused to recycle the outpouring energy. Lk1 AndLk2 ar each composed of alittle leak inductance from the coupled inductance and an external outpouring inductance. 2 freelance management variables, duty cycles d1 and d2, enable the control over 2 ports of the device, whereas the third port is for the ability balance. The fixed-frequency driving signals of the auxiliary switches S3 and S4 ar complementary to primary switch S1. Again, S3 provides a bidirectional path for the battery port. Similarly, S5 is driven in an exceedingly complementary manner to S2. An 180° section shift is applied between the driving signals of S1 and S2.

There ar four operation periods supported the accessible solar energy. First, the sun is within the eclipse stage and also the solar irradiation is either inaccessible or terribly low. This operation amount is outlined as amount one, and also the battery/wind can function the most power supply. Because the sun starts to shine and also the initial solar irradiation is enough for activity a part of the load demand, the operation amount is modified to amount two. The load is provided by each solar and battery/wind power during this period. For period three, the increasing isolation makes the solar energy larger than the load demand. The battery can preserve additional solar energy for backup use. Throughout period four, the charging voltage of the battery reaches the planned level and may be restricted to forestall overcharging.

According to the solar irradiation and also the load demand, the planned three-port device may be operated beneath 2 modes. Within the battery balance mode (mode 1), most electric outlet pursuit (MPPT) is usually operated for the PV port to draw most power from the star panels. The battery port can maintain the ability balance by storing the unconsumed solar energy throughout light-load condition or providing the ability deficit throughout heavy-load condition. The ability sharing of the inputs may be painted as

$$P_{load} = P_{pv} + P_{bat} + P_{wind} \dots\dots\dots(1)$$

Where P_{load} is that the load demand power, P_{pv} is that the PV power underneath solar voltage control, and P_{bat} is that the battery power in mode one, most power is drawn from the PV supply. The battery could offer or absorb power reckoning on the load demand. Therefore, P_{bat} and wind might be either positive or negative. Once the battery charging voltage is more than the utmost setting, the convertors are going to be switched into battery management mode (mode 2). In mode 2, MPPT are going to be disabled; thus, solely a part of the solar energy is drawn. However, the battery voltage might be controlled to guard the battery from overcharging. The ability sharing of the inputs will be depicted as

$$P_{load} = P_{pv} + P_{bat} \dots\dots\dots(2)$$

III. HYBRID WIND-BATTERY-PV SYSTEM FOR AN ISOLATED DC LOAD

The planned hybrid system includes of a WECS and a lead acid battery bank connected inn series with a pv system. The system is intended for a complete dc load. The layout of the complete system together with the management strategy is shown in Fig. 2. The specifications of the WT, SEIG, and battery bank area unit tabulated. The WECS consists of a 4.2-kW horizontal axis WT, gear box with a gear magnitude relation of 1:8 and a five.4 HP SEIG because the WTG. Since the load could be a complete dc load the stator coil terminals of the SEIG ar connected to a condenser bank for self-excitation. The ac output is corrected by three-phase uncontrolled diode rectifier. However, there's a necessity for battery backup to satisfy the load demand throughout the amount of inconvenience of spare wind generation. This hybrid PV- wind-battery system requires suitable control logic for interfacing with the load that already explained above. The uncontrolled dc output of the rectifier is applied to the charge controller circuit of the battery. The charge controller could be 3-port dc-dc convertors that determine the charge and discharging rate of the battery.



International Journal of Advanced Research in Electrical, Electronics and Instrumentation Engineering

(An ISO 3297: 2007 Certified Organization)

Website: www.ijareeie.com

Vol. 6, Issue 5, May 2017

The battery bank connected to the system will either act as a supply or load counting on whether or not it's charging or discharging. However, despite this the battery ensures that the load terminal voltage is regulated. Further, as shown in Fig. 2, the charging of the battery bank is achieved by MPPT logic, whereas the pitch controller limits the mechanical and electrical parameters at intervals the rated price. The integrated action of the battery charge and pitch controller ensures reliable operation of the complete PV-WECS.

IV. CONTROL STRATEGY FOR STAND-ALONE HYBRID W IND-BATTERY SYSTEM

The wind flow is erratic in nature and additionally the solar irradiation. Therefore, a PV-WECS is integrated with the load by means that of AN three port dc-dc convertor to avoid voltage flicker and harmonic generation. The control theme for a complete hybrid pv-wind-battery system includes the charge managementer circuit for battery banks and pitch control logic to make sure WT operation and MPPT to make sure PV operation inside the rated worth. The control logic ensures effective control of the PV and WECS against all attainable disturbances.

V. OPERATION OF THE TOPOLOGICAL MODES

Before activity the analysis, some assumptions ought to be made: 1) within the mean while the because the wind is offered throughout the day endlessly battery are charged by turbine, therefore circuit operation are considered from battery; 2) the magnetizing inductors ar giant enough so this flowing through the inductors is constant; 3) the capacitors ar giant enough so the voltages across the capacitors ar constant. The topological modes over a switch cycle ar shown in Fig. 4 and key waveforms of the projected device ar given in Fig. 5. Careful clarification of every interval is given as follows:

Interval one [see Fig. 3(a), $t_0 \leq t < t_1$]: At t_0 , S1 and auxiliary switches S4 and S5 ar turned OFF, whereas primary switch S2 is turned ON. Though S1 isinthe off state, resonant electrical device Lk1 resonates with Cr1 and Cr4. during this amount, Cr1 is discharged to zero and Cr4 is charged to $V_{bat} + V_{Cc1}$. For the PV port, S2 is turned ON and also the current from the PV panels flows through V_{pv} th – L2 – Lk2 – S2 loop. so as to attain the ZVS feature for S1, the energy hold on in resonant electrical device Lk1 ought to satisfy.

Interval two [see Fig. 3(b), $t_1 \leq t < t_2$]: This mode starts once v_{ds1} is right down to zero. The body diode of S1 is forward biased so the ZVS condition for S1 is established. The resonant current i_{Lk1} is inflated toward zero. L2 continues to be linearly charged during this amount.

Interval three [see Fig. 3(c), $t_2 \leq t < t_3$]: S1 begins to conduct current at t_2 and also the battery port current follows the trail $V_{bat}-L1-Lk1-S1-S2$ isalsoturnedONinthisinterval. Therefore, each L 1 and L2 ar linearly charged and energy of each input ports is hold on in these magnetizing inductors. Auxiliary switches S3,S4, and S5 ar all turned OFF.

Interval four [see Fig. 3(d), $t_3 \leq t < t_4$]: during this interval, S2 starts to be turned OFF and also the auxiliary switch S5 remains within the OFF state. However, a circuit fashioned by Lk2,Cr2, and Cr5 releases the energy hold on in Lk2. Resonant electrical device Cr2 is quickly charged to V_{pv} th + V_{Cc2} , whereas Cr5 is discharged to zero. so as to attain the ZVS feature for S5, the energy hold on in resonant electrical device Lk2 ought to satisfy the subsequent.

Interval five [see Fig. 3(e), $t_4 \leq t < t_5$]: At t_4 , v_{DS5} reaches zero and also the body diode across the auxiliary switch S5 is turned ON. Therefore, a ZVS condition for S5 is established. As long as the Cr5 is far smaller than Cc2, most the magnetizing currents ar recycled to charge the clamp electrical device Cc2. what is more, V_{Cc2} is taken into account as a continuing price since the capacitance of Cc2 is giant enough. This interval ends once electrical device current i_{Lk2} drops to zero.

Interval six [see Fig. 3(f), $t_5 \leq t < t_6$]: At t_5 , this of Lk2 is reversed in direction and energy hold on in t5 is discharged through the Cc2–S5–Lk2–L3 loop. This interval ends once S5 is turned OFF.

International Journal of Advanced Research in Electrical, Electronics and Instrumentation Engineering

(An ISO 3297: 2007 Certified Organization)

Website: www.ijareeie.com

Vol. 6, Issue 5, May 2017

Interval seven [see Fig. 3(g), $t_6 \leq t < t_7$]: Switches S2 and S5 are each within the OFF state at t_6 . A circuit is created by L_{k2} , C_{r2} , and C_{r5} . throughout this interval, C_{r2} is discharged to zero and C_{r5} is charged to $V_{pv} - V_{Cc2}$. to confirm the ZVS shift of S2, the energy hold on in L_{k2} ought to be bigger than the energy hold on in parasitic capacitors C_{r2} and C_{r5}

Interval eight [seeFig.3 (h), $t_7 \leq t < t_8$]: This interval starts when the voltage across Cr2 is zero and also the body diode DS2 is turned ON. Outflow electrical device current i_{Lk2} is linearly inflated and also the secondary-side current of the coupled electrical device is inflated furthermore. The most switch S2 ought to be turned ON before i_{Lk2} becomes positive to confirm ZVS operation.

Interval nine [see Fig. 3(i), $t_8 \leq t < t_9$]: The circuit operation of interval nine is similar to interval three since S1 and S2 are turned ON in each intervals.

Interval ten [Fig.3 (j), $t_9 \leq t < t_{10}$]: At t_9 , S1 is turned OFF, whereas S3 and S4 stay in OFF state. Throughout this interval, Lk1 can resonate with Cr1 and Cr4 to unleash the energy unfree in it. Resonant electrical device Cr1 is charged to $V_{bat} + V_{CC1}$, whereas Cr4 is discharged to zero. To attain the ZVS feature for S4, the energy hold on in resonant electrical device Lk2 ought to satisfy.

Interval eleven [see Fig. 3(k), $t_{10} \leq t < t_{11}$]: This interval begins once vDS4 drops to zero and also the body diode across S4 is turned ON. The ZVS condition for S4 is then established. Most the magnetizing current is recycled to charge Cc1 since Cr4 is far smaller than Cc1. Moreover, VCc1 is taken into account as a continuing price since the capacitance of Cc1 is giant enough. This interval ends once electrical device current iLk1 reaches zero.

Interval twelve [see Fig. 3(l), $t_{11} \leq t < t_{12}$]: this flow through Lk1 is reversed in direction at t_{11} , and also the energy hold on in Cc1 is discharged through the Cc1–S4–Lk1–L1 loop. This interval ends once S4 is turned OFF and also the operation of the projected device over a shift cycle is complete.

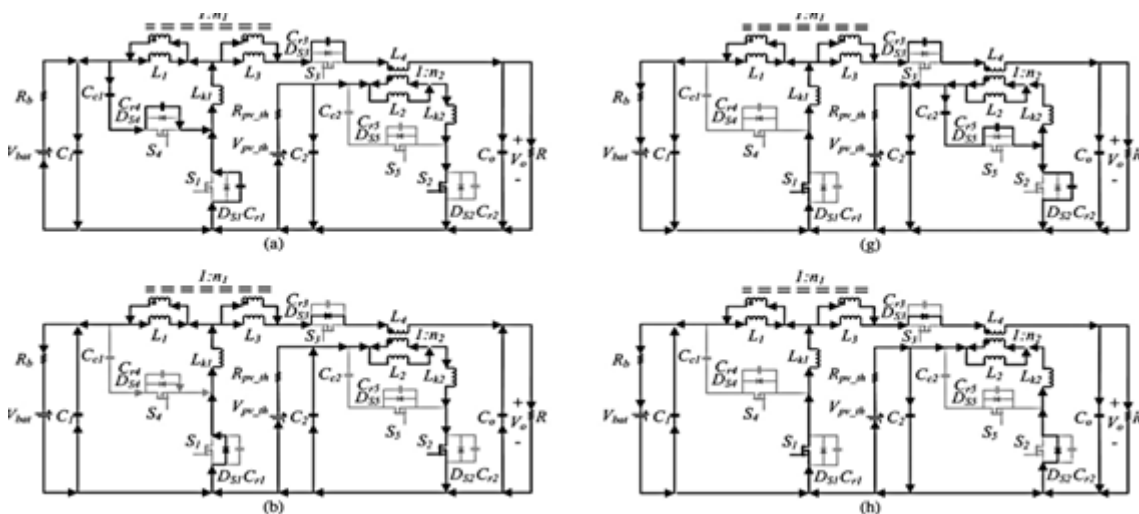


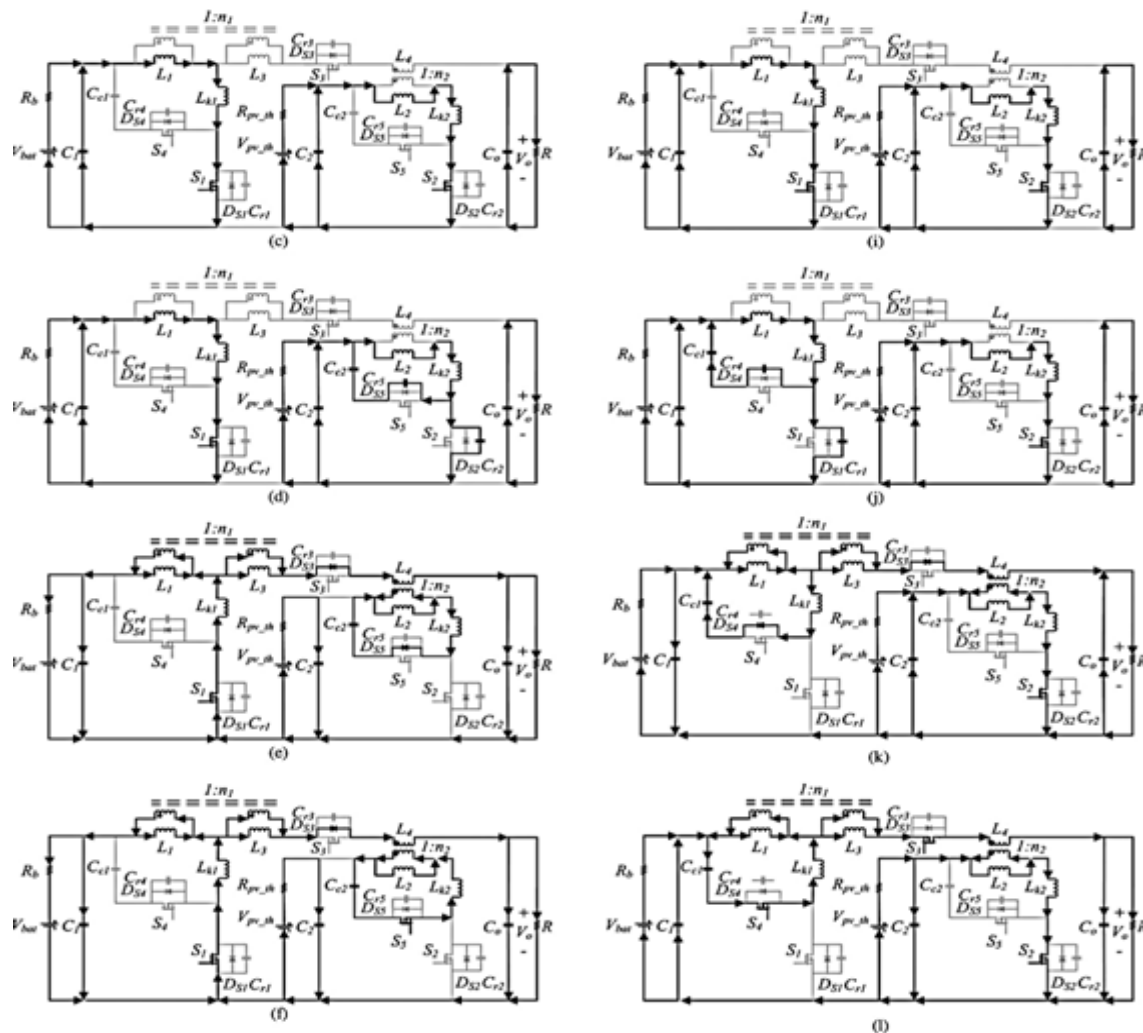
Figure 3 : Modes of operation

International Journal of Advanced Research in Electrical, Electronics and Instrumentation Engineering

(An ISO 3297: 2007 Certified Organization)

Website: www.ijareeie.com

Vol. 6, Issue 5, May 2017



V. RESULT AND DISCUSSION

In the fig 4, it shows the graph of time Vs PV output voltage. Throughput is the average rate of successful message of delivering or tracking maximum power throughout the operation.

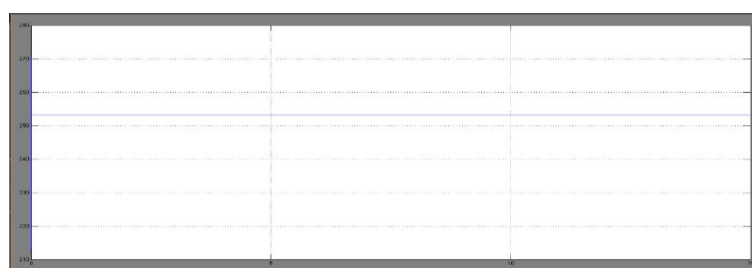


Fig. 4 Simulation time vs PV voltage after MPPT



ISSN (Print) : 2320 – 3765
ISSN (Online): 2278 – 8875

International Journal of Advanced Research in Electrical, Electronics and Instrumentation Engineering

(An ISO 3297: 2007 Certified Organization)

Website: www.ijareeie.com

Vol. 6, Issue 5, May 2017

The below shown figure 5 explains the output voltage of the wind turbine

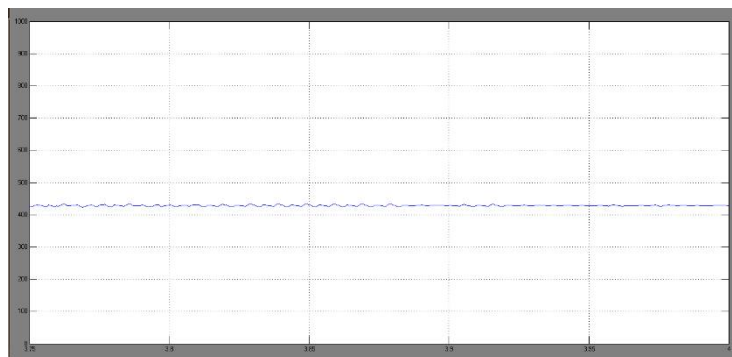


Fig. 5 Simulation time vs Wind voltage

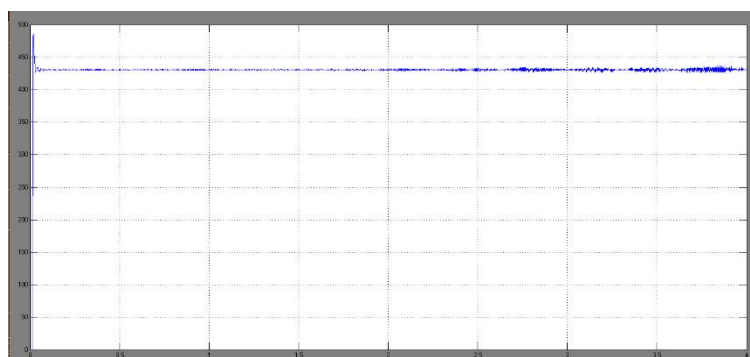


Fig. 6 Battery voltage

In the fig 6, it shows the graph of throughput of Battery voltage Vs time.

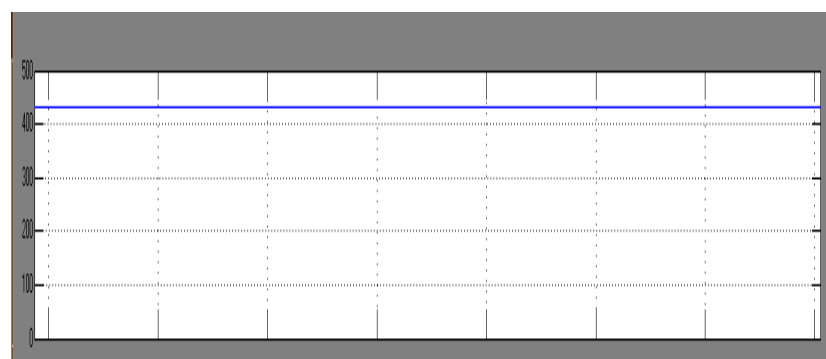


Fig .7Load Voltage



ISSN (Print) : 2320 – 3765
ISSN (Online): 2278 – 8875

International Journal of Advanced Research in Electrical, Electronics and Instrumentation Engineering

(An ISO 3297: 2007 Certified Organization)

Website: www.ijareeie.com

Vol. 6, Issue 5, May 2017

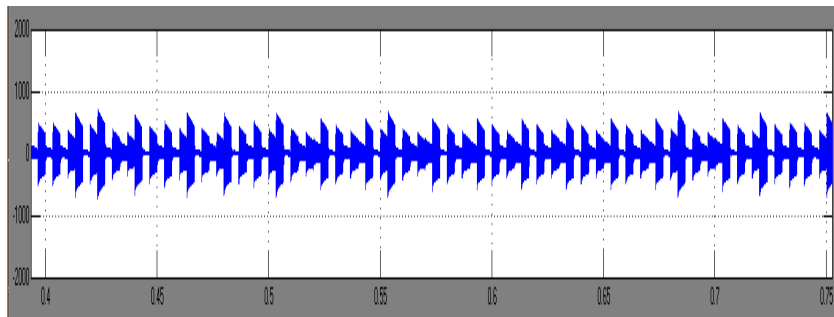


Fig .8 Battery Charging and discharging currents

In Fig 8, the battery charging and discharging for all the time intervals were shown.

VI.CONCLUSION

A high increase three-port DC–DC convertor for complete power systems is planned to integrate solar and wind and battery power. Within the planned topology, 2 coupled inductors are utilized as voltage gain extension cells for prime voltage output applications. 2 sets of buck–boost kind active-clamp circuit's are used to recycle the energy stored in the leakage inductors and improve the efficiency.

The proposed switching strategy only needs to regulate 2 duty ratios in several operation modes. The simulation results validate the practicality of the planned convertor below totally different solar irradiation level with different wind velocities and load demand.

REFERENCES

- [1] A. D. Sahin, "Progress and recent trends in wind energy," *Progress in Energy Combustion Sci.*, vol. 30, no. 5, pp. 501–543, 2004.
- [2] R. D. Richardson and G. M. Mcnerney, "Wind energy systems," *Proc. IEEE*, vol. 81, no. 3, pp. 378–389, Mar. 1993.
- [3] R. Saidur, M. R. Islam, N. A. Rahim, and K. H. Solangi, "A review on global wind energy policy," *Renewable Sustainable Energy Rev.*, vol. 14 , no. 7, pp. 1744–1762, Sep. 2010.
- [4] M. T. Ameli, S. Moslehpur, and A. Mirzale, "Feasibility study for replacing asynchronous generators with synchronous generators in wind farm power stations," in *Proc. IAJC – IJME, Int. Conf. Eng. Technol.*, Music City Sheraton, Nashville, TN, US, ENT paper 129 Nov. 17–19, 2008.
- [5] W. G. Imes and F. D. Rodriguez, "A two-input tri-state converter for spacecraft power conditioning," in *Proc. AIAA Int. Energy Convers. Eng. Conf.*, 1994, pp. 163–168.
- [6] F. D. Rodriguez and W. G. Imes, "Analysis and modeling of a two input DC/DC converter with two controlled variables and four switched networks," in *Proc. AIAA Int. Energy Conf.*, 1994, pp. 163–168.
- [7] B. G. Dobbs and P. L. Chapman, "A multiple-input DC–DC converter topology," *IEEE Power Electron. Lett.*, vol. 1, no. 1, pp. 6–9, Mar. 2003.
- [8] R. J. Wai, Ch. Y. Lin, J. J. Liaw, and Y. R. Chang, "Newly designed ZVS multi-input converter," *IEEE Trans. Ind. Electron.*, vol. 58, no. 2, pp. 555 – 566, Feb. 2011.
- [9] L. Solero, A. Lidozzi, and J. A. Pomilio, "Design of multiple-input power converter for hybrid vehicles," in *Proc. IEEE Appl. Power Electron. Conf.*, 2004, pp. 1145–1151.
- F. Nejabatkhah, S. Danyali, S. H. Hosseini, M. Sabahi, and S. M. Niapour, "Modeling and control of a new three-input DC-DC boost converter for hybrid PV/FC/battery power system," *IEEE Trans. Power Electron.*, vol. 23 , no. 2, pp. 782–792, Mar. 2008.